doi:10.1017/S1431927622009138
Microsc. Microanal. 28 (Suppl 1), 2022

Characterization of Interfaces and Defects in Multiferroic Aurivillius Phase Thin Films by STEM and EELS-SI

Núria Bagués[1*], Louise Colfer[2], Michael Schmidt[2], Lynette Keeney[2], David W. McComb[1,3]

[1.] Center for Electron Microscopy and Analysis, The Ohio State University, Columbus, OH, USA
[2.] Advanced Materials and Surfaces Group, Tyndall National Institute, University College Cork, Lee Maltings Complex, Dyke Parade, Ireland
[3.] Dept. of Material Science and Engineering, Ohio State University, Columbus, Ohio 43212, US
* Corresponding author: baguessalguero.2@osu.edu

Coupling between ferroelectric and ferromagnetic properties in multiferroic materials allows for novel ways of manipulating storage and data information. The Aurivillius phase $Bi_6Ti_xFe_yMn_zO_{18}$ (B6TFMO) system is a rare example of a multiferroic exhibiting room-temperature (RT) properties. For example, thin films of B6TFMO materials possess saturation magnetization (M_S) up to 215 emu/cm^3 [1] and exhibit magnetic-field-induced ferroelectric domain switching at RT. Aurivillius B6TFMO materials offers a naturally layer structured system in layers of 5 ferroelectric perovskite blocks (PK) enclosed between dielectric $(Bi_2O_2)^{2+}$ fluorite-type layers, as presented in Figure 1. Previous reports showed partitioning of magnetic Mn/Fe cations towards the central perovskite layers, which is critical to RT long-range magnetic order [2]. Defects such as out of phase boundaries (OPBs) and stacking faults can influence the extent of magnetic cation partitioning, influencing B6TFMO's multiferroic properties [2,3].

In this work, we combine imaging and spectroscopy techniques to investigate structural defects and interfaces in B6TFMO thin films and their impact on local chemistry. B6TFMO thin films were grown by direct liquid injection chemical vapor deposition (DLI-CVD) on miscut sapphire (0.2^0-10^0) substrates. Direct observation of resultant B6TFMO films is performed using aberration corrected scanning transmission electron microscopy (STEM) in various imaging modes. Figure 2a shows a high angle annular dark field (HAADF)-STEM image confirming the Aurivillius layered structure with OPBs and stacking fault defects. Additionally to these defects previously reported [2], layered antiphase boundaries (APB) are present in some regions of the film. In these regions, the Aurivillius layered structure is replaced by PK enclosed between translational interfaces as shown in Figure 2b. These interfaces are constructed by anatase-like chains of edge-sharing BO_6 octahedra. Nanorod structures were also observed inside PK in these layered APB areas. These type of perovskite-anatase intergrowths and nanorods have previously been reported in similar systems [4-6].

Furthermore, HAADF-STEM imaging is complemented with integrated differential phase contrast (iDPC)-STEM imaging and electron energy loss spectroscopy (EELS) - spectrum imaging (SI). iDPC enables the observation of light elements and reveals the tilted nature of the octahedra within the B6TFMO structure. EELS-SI, using a direct electron detector K2 camera, is performed to further probe magnetic cation environments through the Aurivillius structure and defect regions. Combining these imaging and spectroscopy analysis, with polarization vector mapping, will additionally discuss the influence of interfaces and defects in the local chemistry and ferroelectric behavior within B6TFMO [7].

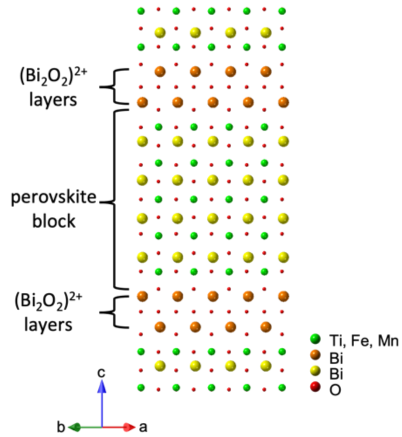

Figure 1. Schematic of the crystal structure of B6TFMO projected down [110].

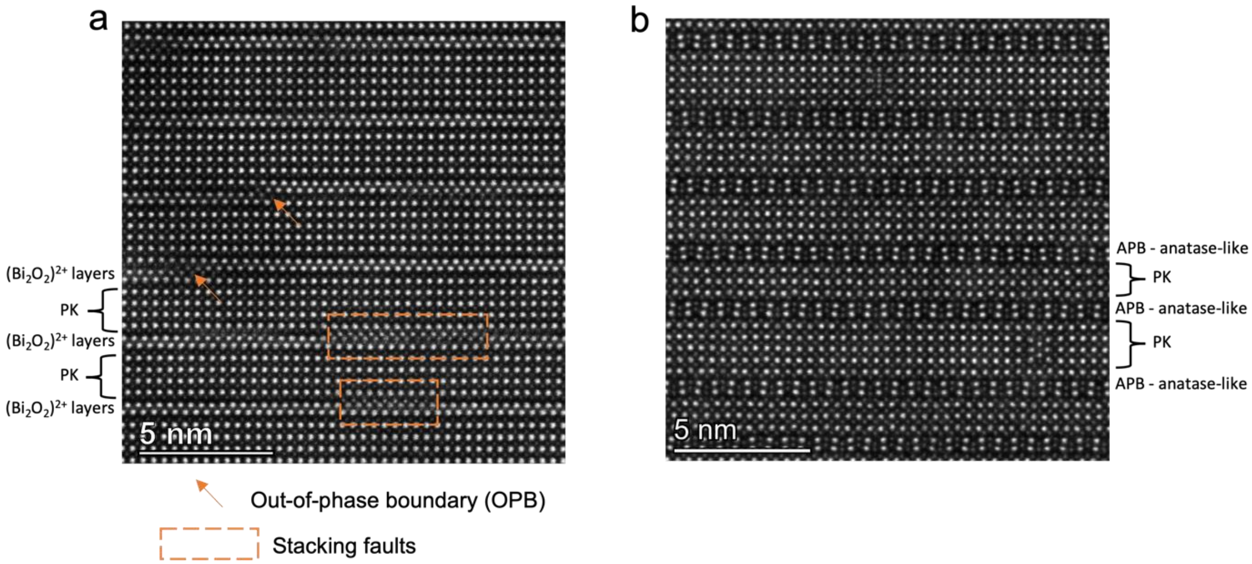

Figure 2. HAADF-STEM images of B6TFMO film along the [110] direction. (a) Region presenting the Aurivillius structure interrupted by OPBs and stacking faults. (b) Region with layered antiphase boundaries (APB), showing perovskite block (PK) – anatase-like layer structure and two nanorods inside the PK. The orange arrows point to the position of the OPBs and the rectangles indicate stacking fault regions.

References:

[1] Faraz, A., et al., J. Am. Ceram. Soc. **100** (2017), p 975– 987. doi:10.1111/jace.14597
[2] Keeney, L., et al., Scientific Reports **7,** 1737 (2017). doi:10.1038/s41598-017-01902-1
[3] Moore, K., et al., ACS Appl. Mater. Interfaces **14(4)** (2022), p 5525-5536. doi:10.1021/acsami.1c17383.
[4] Batuk, D., et al., Inorg. Chem. **55,** 3 (2016), p 1245–1257. doi:10.1021/acs.inorgchem.5b02465
[5] Batuk, D., et al., Inorg. Chem. **56,** 2 (2017), p 931–942. doi:10.1021/acs.inorgchem.6b02559
[6] MacLaren, I., et al., Adv. Funct. Mater., **23** (2013), p 683-689. doi:10.1002/adfm.201201835

https://doi.org/10.1017/S1431927622009138 Published online by Cambridge University Press

[7] The authors acknowledge funding from TNI-OSU/IMR Catalyst-Pilot Program Award. Funding from the Royal Society and Science Foundation Ireland University Research Fellowship URF\R\201008 and Enhancement Award RGF\EA\180206 is gratefully acknowledged. The Electron microscopy was performed at the Center for Electron Microscopy and Analysis (CEMAS) at The Ohio State University.